Asian Journal of Chemistry; Vol. 38, No. 7 (2026), 1890-1896
ASIAN JOURNAL OF CHEMISTRY
https://doi.org/10.14233/ajchem.2026.36113

In situ Synthesis of Zinc Oxide Nanoparticles on Cotton Fabric for Eco-Friendly Textile Applications

K.V. ARUNKUMAR[1], K.M. PACHIYAPPAN[1], A. GANDAMALLA[2] and D. MANIKANDAN[3,*]

[1]Department of Costume Design and Fashion, PSG College of Arts and Science, Coimbatore-641014, India
[2]Chemical Engineering and Process Technology Department, CSIR-Indian Institute of Chemical Technology, Tarnaka, Hyderabad-500007, India
[3]Department of Chemistry (SF), PSG College of Arts and Science, Coimbatore-641014, India

Corresponding author: E-mail: manikandandhayalan88@gmail.com

Received: 1 April 2026 *Accepted*: 15 June 2026 *Published online*: 3 July 2026 AJC-22414

This study describes the fabrication of cotton twill fabrics coated with zinc oxide nanoparticles (ZnO NPs) for the development of eco-friendly textiles. ZnO NPs were synthesized *in situ* on citric acid-pretreated cotton fabrics using zinc acetate as the precursor and sodium hydroxide as the alkaline agent. Citric acid pretreatment enhanced zinc ion adsorption, enabling uniform nanoparticle deposition and strong interfacial bonding between the ZnO NPs and cellulose fibers under controlled alkaline and thermal conditions. FT-IR analysis confirmed the formation of ZnO NPs through characteristic absorption bands at 500-430 cm^{-1}. EDX analysis confirmed the presence of zinc and oxygen, while FESEM images revealed a homogeneous nanoscale distribution of the nanoparticles on the fabric surface. XRD analysis confirmed the cellulose-I crystalline structure together with weak diffraction peaks corresponding to partially amorphous ZnO NPs. The functionalized fabrics exhibited concentration-dependent antibacterial activity, demonstrating enhanced antimicrobial performance with increasing ZnO loading. The proposed *in situ* synthesis method provides a simple, durable and effective approach for the functionalization of cotton fabrics, offering promising potential for protective and healthcare textile applications.

Keywords: ZnO nanoparticles, Cotton fabric, Antimicrobial textile eco-functional finishing nanotechnology, Sustainable textiles.

INTRODUCTION

The incorporation of nanotechnology into textiles has provided beneficial antimicrobial, UV protective, self-cleaning and durable multifunctional fabrics, which have positively impacted the textile industry [1]. Zinc oxide nanoparticles (ZnO NPs) possess unique physico-chemical properties including excellent UV-shielding ability, photocatalytic activity, chemical stability and broad-spectrum antimicrobial efficacy, making them attractive for a wide range of applications [2,3]. In addition, ZnO NPs are considered eco-friendly and biocompatible, further enhancing their suitability for protective textile applications [4]. Cotton fabric is an ideal substrate for ZnO functionalization owing to its high cellulose content and the abundance of hydroxyl groups, which facilitate metal-ion adsorption and promote the nucleation and growth of ZnO NPs on the fiber surface [5]. Consequently, the *in situ* synthesis of ZnO NPs on cotton textiles provides an effective strategy for achieving uniform nanoparticle deposition, improving interfacial adhesion and enhancing the durability of the functional properties imparted by the ZnO coating [6].

Conventional *ex situ* techniques, such as dip-pad-dry-cure and sol-gel coating, are widely employed to deposit ZnO NPs onto cotton fabrics [7]. Although these methods impart excellent antimicrobial and UV-protective properties, the nanoparticles are primarily confined to the fabric surface, resulting in the weak adhesion, particle agglomeration and progressive coating loss after repeated laundering [8,9]. Consequently, the functional performance of the coated fabrics deteriorates over time, limiting their long-term practical application.

To overcome these limitations, *in situ* synthesis of ZnO NPs within textile fibers has emerged as a promising alternative. In this approach, nanoparticle nucleation and growth occur directly on the fiber surface under controlled reaction conditions, promoting uniform dispersion and stronger interfacial interactions with the cellulose matrix [10,11]. The formation of hydrogen and/or covalent bonds between ZnO NPs and cellulose enhances nanoparticle anchoring, minimises agglo-

meration and significantly improves the durability of the antimicrobial coating. Moreover, *in situ* nucleation provides a more homogeneous nanoparticle distribution than conventional surface-coating techniques [12].

Among the available synthesis routes, alkaline precipitation is a simple and effective method for the *in situ* formation of ZnO NPs. In this process, Zn^{2+} ions react with hydroxide ions to form zinc hydroxide intermediates, which are subsequently converted into crystalline ZnO during thermal treatment [13]. This strategy enables controlled nanoparticle growth while ensuring strong attachment to the cotton fibers. In addition to their excellent UV-blocking capability arising from a wide band gap, ZnO NPs exhibit broad-spectrum antimicrobial activity through the generation of reactive oxygen species (ROS), disruption of microbial cell membranes and the release of Zn^{2+} ions [14,15].

Although numerous studies have reported ZnO-coated cotton fabrics, limited attention has been given to the *in situ* synthesis of ZnO nanoparticles on cotton twill fabrics using citric acid activation followed by controlled alkaline precipitation. Citric acid pretreatment introduces additional carboxyl groups onto the cellulose surface, enhancing zinc ion adsorption and promoting stronger anchoring and more uniform distribution of ZnO NPs [16]. Therefore, the present study aims to develop a controlled in situ synthesis strategy for ZnO-functionalized cotton twill fabrics through citric acid activetion, zinc acetate impregnation and NaOH-assisted alkaline precipitation [17]. The structural, morphological and compositional properties of the functionalized fabrics were characterised using FT-IR, FESEM, EDX and XRD, while antimicrobial assays were performed to evaluate their functional performance.

EXPERIMENTAL

All the chemicals used were of analytical grade and used as received without purification. Scoured and bleached 100% cotton twill weave fabrics were used as substrates to remove impurities and provide uniform chemical absorption. For the purpose of activating cellulose surfaces by increasing reactive binding sites, citric acid (analytical grade) was used as the activating agent. Zinc acetate dihydrate was employed as the zinc source and 1 M NaOH was used as the alkaline precipitant for the *in situ* synthesis of ZnO NPs. In order to prevent contamination by ions, only distilled water was used.

Synthesis of ZnO nanoparticles

Treatments with citric acid: Cotton fabrics were pretreated with citric acid in order to enhance the *in situ* nucleation and the subsequent zinc ion adsorption. Citric acid solution was prepared by dissolving 0.5 g of citric acid in 100 mL of distilled water [18]. The fabric samples were immersed to ensure complete penetration into the cellulose matrix. Citric acid acts as a chelating and mild crosslinking agent, introducing additional carboxyl groups that facilitate Zn^{2+} ion adsorption, thereby enhancing metal ion uptake and promoting uniform nucleation of ZnO NPs during subsequent impregnation [19,20].

Zinc acetate impregnation: The citric acid-treated fabrics were immersed in 0.25 M or 0.5 M zinc acetate solution and placed in a reaction vessel on a magnetic stirrer to facilitate uniform diffusion of Zn^{2+} ions into the cellulose fibers [21]. The reaction was carried out at 80 ºC with continuous stirring at 800 rpm for 30 min, providing optimal conditions for Zn^{2+} interaction with the hydroxyl and carboxyl groups of the activated cellulose [22]. Continuous agitation ensured uniform metal ion adsorption throughout the fabric. Following zinc acetate impregnation, the fabrics were immediately transferred to an alkaline solution to initiate the precipitation and *in situ* formation of ZnO NPs [23].

***In situ* formation of ZnO NPs:** Fabrics, after zinc acetate impregnation, were treated with a 1 M NaOH solution, added dropwise and under constant stirring to induce a gradual increase of pH. The precipitation of zinc hydroxide, was localised (within and on the surface of the cotton fibers) to correspond with the increment of pH and its opacity signified the onset of $Zn(OH)_2$ nucleation within the solution [24]. When the temperature was kept constant at 80 ºC, the zinc hydroxide intermediate was thermally dehydrated to yield ZnO NPs. As Zn^{2+} ions had already diffused into the cellulose matrix during the impregnation step, nucleation and growth of ZnO NPs occurred directly on the fiber surface. This *in situ* process promoted strong nanoparticle anchoring enhanced interactions with cellulose hydroxyl groups and minimized particle agglomeration [25]. After completion of the reaction, the functionalized fabric samples were collected for subsequent characterisation and analysis.

Autoclaving and drying: The composite samples were subjected to autoclaving under controlled hydrothermal conditions to increase the ZnO NPs crystallinity and fixation. This process also converted the residual zinc hydroxide to crystalline ZnO NPs and enhanced the bond strength between the ZnO NPs and the fibers [26]. After autoclaving, the samples were treated to a thorough rinse with distilled water to remove any loosely attached particles, leaving only strongly bonded ZnO NPs to the fabric, which increased durability. Finally, the fabrics were air-dried at room temperature to prevent thermal degradation and stored in a clean, moisture-free environment prior to characterisation.

Antimicrobial activity: The antibacterial activity of untreated and ZnO NPs-coated cotton fabrics against *Staphylococcus aureus* was evaluated using the agar diffusion method. A fresh bacterial culture was prepared in nutrient broth and adjusted to an optical density (OD_{600}) of approximately 0.15, corresponding to the 0.5 McFarland standard. Sterile Mueller-Hinton agar (MHA) plates were uniformly inoculated to obtain a bacterial lawn. Untreated cotton fabric (control, C) and ZnO NPs-coated fabrics prepared using 0.25 M and 0.5 M zinc acetate solutions (C1 and C2, respectively) were cut into 1 cm × 1 cm sterile pieces and aseptically placed on the inoculated agar surface. The plates were incubated at 37 ºC for 24 h under aerobic conditions. Antibacterial activity was assessed by measuring the zone of inhibition surrounding each fabric sample, with larger inhibition zones indicating greater antibacterial efficacy. The performance of the treated fabrics was compared with that of the untreated control.

RESULTS AND DISCUSSION

FT-IR studies: The FT-IR spectra of untreated cotton (C) and ZnO NPs-coated cotton fabrics prepared using 0.25

M and 0.5 M zinc acetate are shown in Fig. 1. The spectra are dominated by the characteristic absorption bands of cellulose, reflecting the high cellulose content of cotton. Any shifts in peak position or changes in intensity after ZnO loading indicate interactions between ZnO NPs and the functional groups of cellulose. The untreated cotton exhibited a broad absorption band at 3600-3200 cm^{-1} (centered at ~3330 cm^{-1}), corresponding to O–H stretching vibrations of hydrogen-bonded hydroxyl groups. The bands at 2890-2850 cm^{-1} and ~2900 cm^{-1} were assigned to the symmetric and asymmetric C–H stretching vibrations of CH and CH_2 groups in the cellulose glucose units. The absorption band at 1650-1630 cm^{-1} was attributed to the H–O–H bending vibration of absorbed water, while the bands within the 1200-1000 cm^{-1} region corresponded to C–O–C and C–O stretching vibrations characteristic of the cellulose backbone. Following ZnO NPs deposition, slight changes in band intensity together with the appearance of a characteristic Zn–O absorption band in the 500-430 cm^{-1} region confirmed the successful formation of ZnO NPs on the cotton fibers. The cellulose absorption bands remained largely unchanged indicating that the crystalline cellulose structure was preserved during the functionalization process. Furthermore, the absence of additional absorption bands suggests that no secondary phases or impurity compounds were formed.

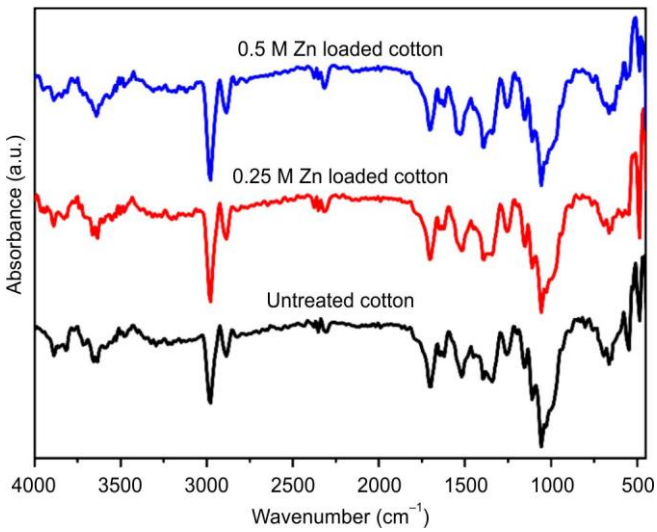

Fig. 1. FT-IR analysis of untreated cotton, 0.25 M Zn loaded and 0.5 M Zn loaded

XRD studies: The crystalline structure of untreated cotton and ZnO NPs-coated cotton fabrics was investigated by XRD and the diffraction patterns are shown in Fig. 2. All samples exhibited the characteristic diffraction peaks of cellulose-I, indicating that the intrinsic crystalline structure of cotton was preserved after ZnO NP deposition. The untreated cotton showed prominent reflections at $2\theta \approx 14.5^{\circ}$, 16.5º and 22.6º, corresponding to the $(1\,\bar{1}0)$, (110) and (200) crystallographic planes, respectively. The intense peak at 22.6º, assigned to the (200) plane, represents the ordered packing of cellulose chains within the microfibrils, while the weak reflection at 34-35º corresponds to the (004) plane.

Following ZnO NPs deposition, the characteristic cellulose reflections remained unchanged, confirming that the

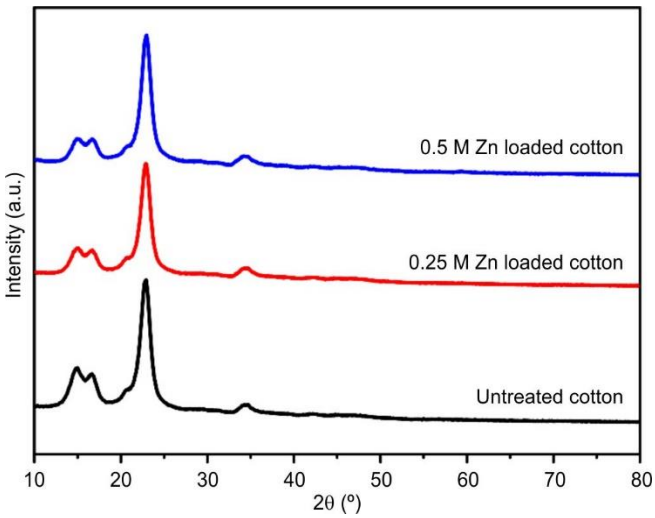

Fig. 2. XRD analysis of untreated cotton, 0.25 M Zn loaded and 0.5 M Zn loaded

functionalisation process did not disrupt the cellulose crystalline framework. For the 0.25 M ZnO-coated fabric, a slight increase in the intensity of the (200) reflection was observed, suggesting improved ordering of the cellulose microfibrils due to interactions between Zn^{2+} species and the hydroxyl groups of cellulose, which act as nucleation sites for ZnO formation. Increasing the zinc precursor concentration to 0.5 M resulted in a further enhancement of peak intensity with slight peak broadening, indicating greater ZnO loading and stronger interactions with the cellulose matrix. Weak diffraction peaks appearing in the 31-36º region were attributed to nanocrystalline ZnO, although their low intensity reflects the small crystallite size and uniform dispersion of the nanoparticles within the cellulose matrix.

The XRD results demonstrate that ZnO NPs were successfully deposited on the cotton fibers without altering the native cellulose-I crystalline structure. The preservation of the cellulose diffraction peaks, together with the appearance of weak ZnO reflections, confirms the successful formation of nanocrystalline ZnO on the fiber surface. These findings are consistent with the FT-IR results, which revealed the characteristic Zn–O stretching vibration, indicating that ZnO NPs were anchored to the cellulose matrix through interactions between ZnO and the hydroxyl groups of cellulose, thereby ensuring uniform deposition while preserving the structural integrity of the cotton fibers.

FESEM-EDX: The surface morphology and elemental composition of untreated and ZnO NPs-coated cotton fabrics were examined using FESEM and EDX, and the results are shown in Figs. 3-5. The untreated cotton (C sample) exhibited the characteristic morphology of natural cellulose fibers, with smooth, continuous and clean fibrillar surfaces free from particulate deposits or structural defects (Fig. 3). The corresponding EDX spectrum contained only carbon and oxygen peaks, confirming the cellulose composition and the absence of zinc or other inorganic species. These observations provide the reference morphology and elemental composition of the untreated fabric.

After *in situ* treatment with 0.25 M zinc acetate (C1 sample), noticeable changes in surface morphology were obs-

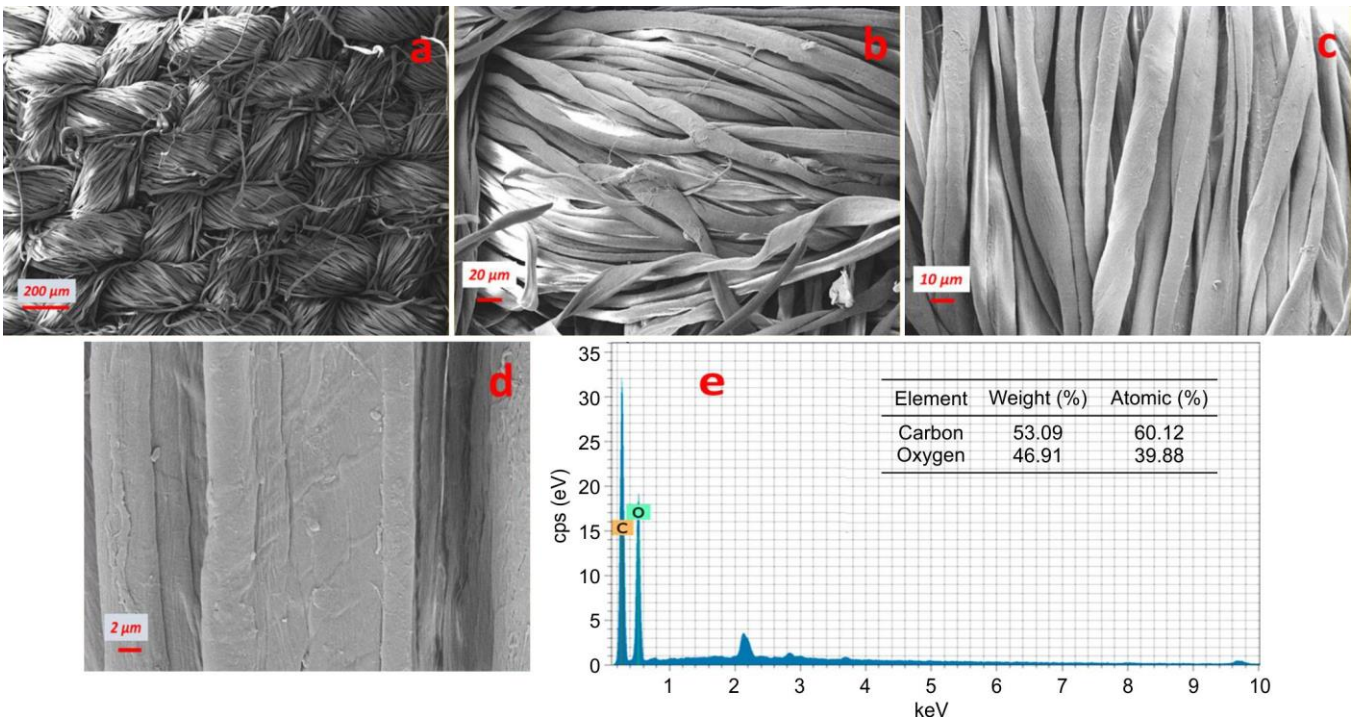

Fig. 3. SEM analysis of untreated cotton with different magnifications (a-d), EDX and respective elemental and atomic percentages of untreated cotton (e)

erved (Fig. 4). FESEM images showed uniformly distributed ZnO NPs on the fiber surface with predominantly spherical to slightly hexagonal morphology and only limited particle aggregation. The hydroxyl-rich cellulose surface served as an effective nucleation site, promoting controlled growth and homogeneous dispersion of ZnO NPs. The corresponding EDX spectrum displayed characteristic Zn-Lα (~1 keV) and Zn-Kα (8.6-9.0 keV) peaks in addition to the carbon and oxygen signals, confirming successful ZnO deposition while preserving the cellulose framework.

When the zinc acetate concentration was increased to 0.50 M (C2), the density of ZnO NPs on the fiber surface increased considerably (Fig. 5). A more continuous nanoparticle coating was observed, accompanied by partial particle aggregation resulting from the higher precursor concentration and faster nucleation rate. Despite the greater ZnO loading, the fibrous morphology of cotton remained unchanged indicating that the synthesis conditions did not affect the structural integrity of the cellulose fibers. The stronger zinc signals observed in the EDX spectrum of C2 sample further verified the higher amount of ZnO deposited on the fabric surface.

The FESEM observations are consistent with the EDX results, where increasing zinc precursor concentration produced progressively stronger zinc signals confirming concentration-dependent ZnO loading. This behaviour also agrees with the FT-IR spectra, which showed the characteristic Zn–O stretching vibration and the XRD patterns, which confirmed the preservation of the cellulose-I crystalline structure after nanoparticle deposition. The higher surface coverage obtained with the 0.50 M precursor corresponded to enhanced antibacterial activity, indicating that the amount and distribution of ZnO NPs on the cotton fibers play an important role in determining the functional performance of the treated fabric.

ZnO loading percentage on cotton fabric: The amount of ZnO nanoparticles deposited on the cotton fabric was estimated from the percentage weight gain before and after the *in situ* synthesis process. The untreated cotton fabric (C) showed no measurable change in weight, whereas the ZnO-treated samples exhibited a clear increase, confirming successful nanoparticle deposition. Sample C1, prepared using 0.25 M zinc acetate, increased in weight from 25.0 g to 26.1 g, corresponding to a 4.4% weight gain. In contrast, sample C2, prepared with 0.50 M zinc acetate, showed a weight increase from 25.0 g to 27.3 g, representing a 9.2% gain. The higher weight gain obtained for C2 indicates that increasing the precursor concentration promotes greater ZnO NPs deposition on the cotton fibers. This observation agrees with the FESEM micrographs, which revealed a higher nanoparticle density on the fiber surface at 0.50 M and with the EDX results, where the zinc content increased from 5.29 wt.% for C1 to 18.62 wt.% for C2 (Table-1). Thus, the weight gain, morphological observations and elemental analysis consistently confirm concentration-dependent loading of ZnO NPs on the cotton substrate through the *in situ* synthesis process.

TABLE-1
WEIGHT GAIN PERCENTAGE OF
UNTREATED AND ZnO TREATED COTTON FABRICS

Sample	ZnO conc. (M)	Fabric weight (g)		Increase (%)
		Before	After	
C	0	25	25.0	–
C1	0.25	25	26.1	4.4
C2	0.50	25	27.3	9.2

Antimicrobial activity: The antibacterial activity of untreated and ZnO NPs-coated cotton fabrics against *S. aureus*

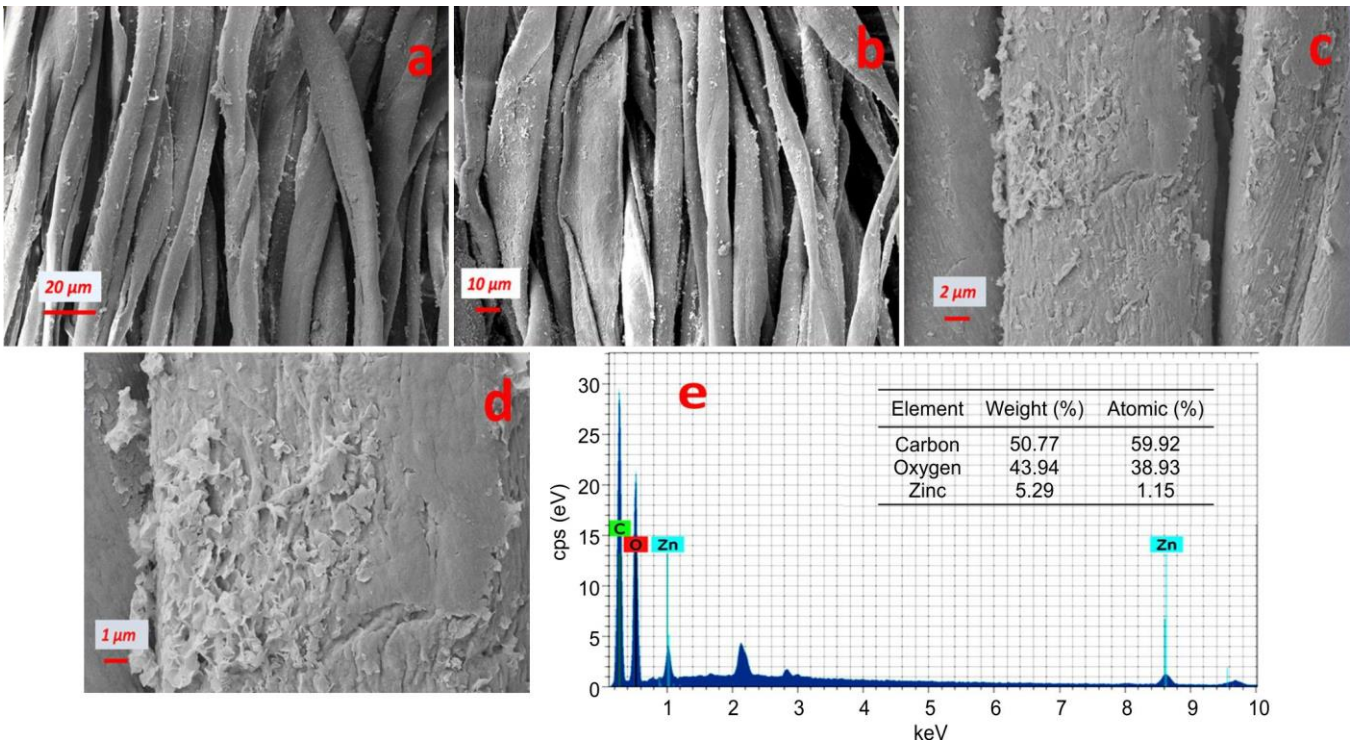

Fig. 4. SEM analysis of 0.25 M Zn-loaded cotton with different magnifications (a-d), EDX and respective elemental and atomic percentages of untreated cotton (e)

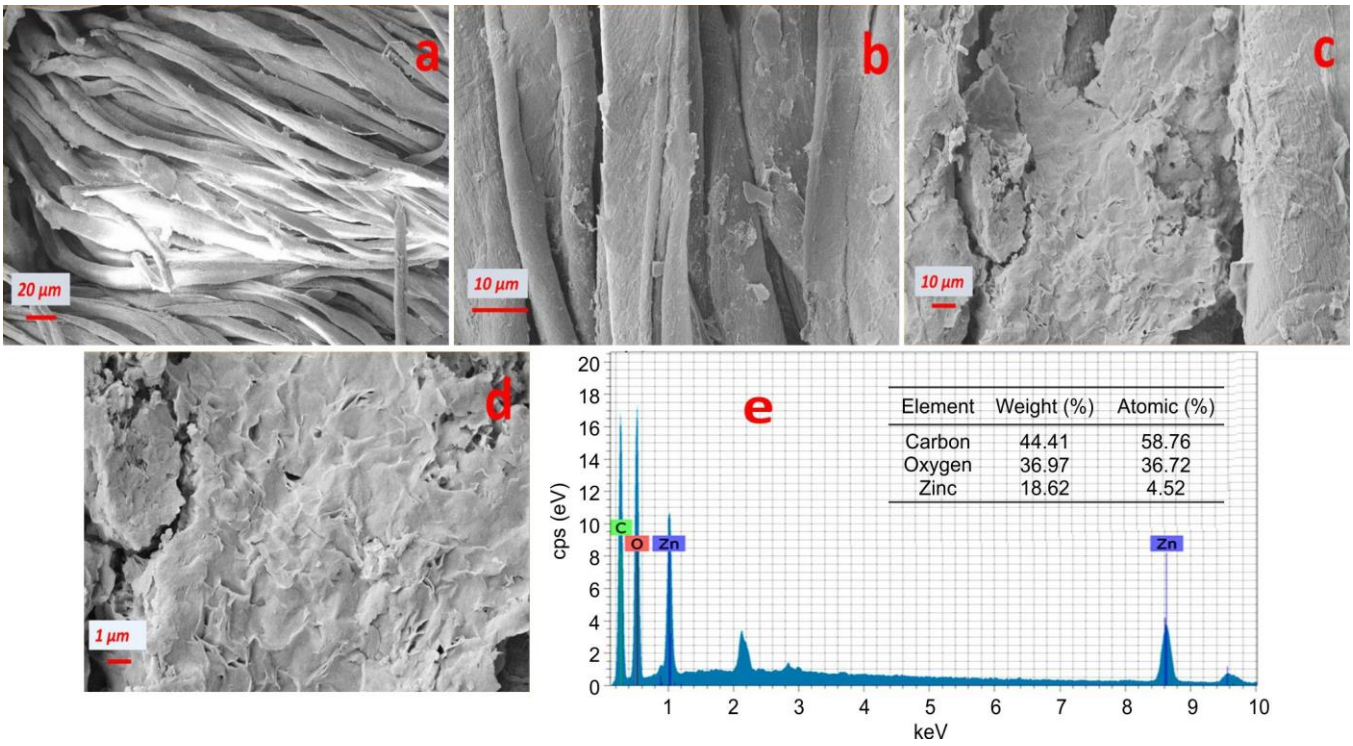

Fig. 5. SEM analysis of 0.5 M Zn-loaded cotton with different magnifications (a-d), EDX and respective elemental and atomic percentages of untreated cotton (e)

was evaluated using the agar diffusion method and the results are shown in Fig. 6. The untreated cotton fabric (C) exhibited dense bacterial growth surrounding the sample without any visible inhibition zone, indicating that native cotton fibers do not possess inherent antibacterial activity.

In contrast, both ZnO-treated fabrics inhibited bacterial growth, confirming the successful incorporation of antimicrobial functionality through the *in situ* synthesis process. The fabric prepared using 0.25 M zinc acetate (C1) produced a partial inhibition zone with a measured diameter of 2.67 ±

Fig. 6. Antimicrobial activity of untreated cotton (C) and ZnO-treated samples (C1 and C2)

0.58 mm, whereas the sample prepared using 0.50 M zinc acetate (C2) exhibited a well-defined inhibition zone of 8.33 ± 0.58 mm. The larger inhibition zone observed for C2 indicates that antibacterial activity increased with increasing ZnO NPs loading (Table-2). The enhanced antibacterial performance of the treated fabrics is attributed to the antimicrobial mechanisms of ZnO NPs, including the generation of ROS, direct disruption of bacterial cell membranes through nanoparticle–cell interactions and the release of Zn^{2+} ions that interfere with essential cellular processes. Increasing the ZnO content provides a larger number of active antimicrobial sites on the fiber surface, thereby improving bacterial inhibition.

TABLE-2
ANTIMICROBIAL ACTIVITY

Sample	Conc. (M)	Zone (mm)	Mean ± SD
C	0	0	0 ± 0
C1	0.25	3, 2, 3	2.67 ± 0.58
C2	0.50	8, 9, 8	8.33 ± 0.58

The antibacterial results are consistent with the FESEM and EDX analyses. FESEM images showed a progressive increase in nanoparticle coverage as the precursor concentration increased from 0.25 M to 0.50 M, while EDX confirmed the corresponding increase in zinc content on the cotton surface. The higher nanoparticle loading observed for C2 provided higher surface contact with bacterial cells, resulting in superior antibacterial performance. These results demonstrate that precursor concentration directly influences ZnO NPs deposition and consequently, the antimicrobial efficiency of the functionalized cotton fabrics.

Ultraviolet (UV) protection performance: The UV protective performance of untreated and ZnO NPs-coated cotton fabrics was evaluated according to AATCC 183 and the results are shown in Table-3. The untreated cotton fabric exhibited a UPF value of 15.20 ± 0.36, corresponding to moderate UV protection. Following *in situ* ZnO deposition, the UV-blocking performance improved markedly. The fabric treated with 0.25 M zinc acetate (C1) showed the highest UPF value of 22.55 ± 1.17, while the 0.50 M sample (C2) exhibited a UPF of 20.46 ± 1.61. The enhanced UV protection is attributed to the wide band gap of ZnO nanoparticles, which efficiently absorb and scatter ultraviolet radiation, thereby reducing UV transmission through the fabric. UV-A protection increased from 91.39% for untreated cotton to 93.69% (C1) and 93.34% (C2), whereas UV-B protection improved from 94.77% to 96.48% and 96.11%, respectively. These results confirm that *in situ* deposition of ZnO NPs significantly enhances the UV-protective properties of cotton fabrics without requiring additional finishing treatments.

TABLE-3
UV PROTECTION ANALYSIS

Sample	UPF (Mean ± SD)	Blocking (%)	
		UV-A	UV-B
C	15.20 ± 0.36	91.39	94.77
C1	22.55 ± 1.17	93.69	96.48
C2	20.46 ± 1.61	93.34	96.11

Air permeability of ZnO-coated cotton fabrics: The air permeability of untreated and ZnO NPs-coated cotton fabrics was evaluated to determine the effect of nanoparticle deposition on fabric breathability. The untreated cotton exhibited an air permeability of 125 ± 3, which decreased to 115 ± 3 for the 0.25 M ZnO NPs-coated sample (C1) and 110 ± 3 for the 0.50 M sample (C2). The reduction in air permeability is attributed to partial filling of the inter-fiber pores by ZnO NPs, which restricts airflow through the fabric. The higher decrease observed for C2 is consistent with the higher ZnO NPs loading confirmed by the FESEM and EDX analyses. Despite this reduction, both ZnO NPs-coated fabrics retained good air permeability indicated that the *in situ* functionalisation process enhanced the protective properties of the cotton fabric without significantly com-promising its breathability.

Tensile strength of ZnO-coated cotton fabrics: Table-4 presents the tensile strength of untreated and ZnO NPs-coated cotton fabrics in both the warp and weft directions. The untreated cotton exhibited tensile strengths of 121 lbs (warp) and 72 lbs (weft). Following ZnO NPs deposition, a slight reduction in tensile strength was observed. Sample C1 showed warp and weft strengths of 116 lbs and 64 lbs, respectively, while sample C2 exhibited values of 109 lbs and 59 lbs. The decrease in tensile strength is attributed to the chemical treatment and the deposition of ZnO NPs on the fiber surface, which may slightly alter the fiber structure. Nevertheless, the reduction was limited, and the treated fabrics retained good mechanical integrity after in situ functionalization. These results indicate that *in situ* ZnO NPs deposition enhances the functional properties of cotton fabrics while preserving their mechanical performance to a large extent.

TABLE-4
TENSILE STRENGTH OF ZnO-COATED COTTON FABRICS

Sample	Warp (lbs)	Weft (lbs)
C	121	72
C1	116	64
C2	109	59

Conclusion

In this study, ZnO NPs were successfully synthesized *in situ* on cotton twill fabric through citric acid activation, zinc acetate impregnation and controlled alkaline precipitation. The proposed method promoted direct nucleation and growth of ZnO NPs on the cellulose fiber surface while preserving the native cellulose I crystalline structure. FT-IR confirmed the formation of Zn–O bonds, whereas FESEM and EDX analyses verified uniform, concentration-dependent nanoparticle deposition and increasing zinc content with higher precursor concentrations. XRD analysis further supported the successful formation of nanocrystalline ZnO without disrupting the structural integrity of the cotton fibers. The functionalized fabrics exhibited enhanced antibacterial activity and improved UV protection, with the highest performance achieved at the greater ZnO loading, while maintaining good air permeability and mechanical strength. These results demonstrate that the *in situ* synthesis approach provides a simple, scalable, and durable route for producing multifunctional ZnO NPs-coated cotton fabrics with potential applications in medical, protective and hygienic textiles.

ACKNOWLEDGEMENTS

The authors express their sincere thanks to their respective College Management of Department of Costume Design and Fashion, PSG College of Arts and Science, Coimbatore, India, providing the necessary requirements for this research work.

CONFLICT OF INTEREST

The authors declare that there is no conflict of interests regarding the publication of this article.

DECLARATION OF AI-ASSISTED TECHNOLOGIES

During the preparation of this manuscript, the authors used an AI-assisted tool(s) to improve the language. The authors reviewed and edited the content and take full responsibility for the published work.

REFERENCES

1. J. Ghosh, N.S. Rupanty, T. Noor, T.R. Asif, T. Islam and V. Reukov, *RSC Adv.*, **15**, 10984 (2025); https://doi.org/10.1039/D5RA01429H
2. E.L. Irede, R. F. Awoyemi, B. Owolabi, O.R. Aworinde, R.O. Kajola, A. Hazeez, A.A. Raji, L.O. Ganiyu, C.O. Onukwuli, A.P. Onivefu and I.H. Ifijen, *RSC Adv.*, **14**, 20992 (2024); https://doi.org/10.1039/d4ra02452d
3. S.K.S. Kumar, C. Prakash, P. Ramesh, N. Sukumar and N.K. Palaniswamy, *J. Nat. Fibers*, **18**, 2302 (2021); https://doi.org/10.1080/15440478.2020.1726241
4. R. Mohammadipour-Nodoushan, S. Shekarriz, Z. Shariatinia, M. Heydari and M. Montazer, *Int. J. Biol. Macromol.*, **242**, 124916 (2023); https://doi.org/10.1016/j.ijbiomac.2023.124916
5. M.Q. He, Y. Ai, W. Hu, L. Guan, M. Ding and Q. Liang, *Adv. Mater.*, **35**, 2211915 (2023); https://doi.org/10.1002/adma.202211915
6. M. Rajalakshmi, S. Kubera Sampath Kumar, D. Vasanth Kumar, M. Siva Jagadish Kumar and C. Prakash, *Sci. Rep.*, **12**, 9441 (2022); https://doi.org/10.1038/s41598-022-13661-9
7. Y. Wang, V. Baheti, M.Z. Khan, M. Viková, K. Yang, T. Yang and J. Militký, *J. Textile Institute*, **113**, 2238 (2022); https://doi.org/10.1080/00405000.2021.1975905
8. S. Sfameni, M. Hadhri, G. Rando, D. Drommi, G. Rosace, V. Trovato and M.R. Plutino, *Inorganics*, **11**, 19 (2023); https://doi.org/10.3390/inorganics11010019
9. K. Saravanan, S.K. Sampath Kumar, C. Prakash, S. Sivamani, J. Prakash Maran and G. Rajeshkumar, *J. Nat. Fibers*, **19**, 10846 (2022); https://doi.org/10.1080/15440478.2021.2002774
10. G. Montes-Hernandez, M. Di Girolamo, G. Sarret, S. Bureau, A. Fernandez-Martinez, C. Lelong and E. Eymard Vernain, *ACS Omega*, **6**, 1316 (2021); https://doi.org/10.1021/acsomega.0c04814
11. S.A. Jadhav, A.H. Patil, S.S. Thoravat, V.S. Patil and P.S. Patil, *Nanobiotechnol. Reports*, **16**, 543 (2021); https://doi.org/10.1134/S2635167621040170
12. T.I. Shaheen, M.E. El-Naggar, A.M. Abdelgawad and A. Hebeish, *Int. J. Biol. Macromol.*, **83**, 426 (2016); https://doi.org/10.1016/j.ijbiomac.2015.11.003
13. N. Gorodylova, S. Cousy, P. Šulcová and L. Svoboda, *J. Therm. Anal. Calorim.*, **127**, 675 (2017); https://doi.org/10.1007/s10973-016-5517-4
14. R.K. Dutta, B.P. Nenavathu, M.K. Gangishetty and A.V. Reddy, *Colloids Surf. B Biointerfaces*, **94**, 143 (2012); https://doi.org/10.1016/j.colsurfb.2012.01.046
15. B. Saha, A. Saha, P. Das, A. Kakati, A. Banerjee and P. Chattopadhyay, *Heliyon*, **10**, e40027 (2024); https://doi.org/10.1016/j.heliyon.2024.e40027
16. E.F. Aboelfetoh, M.E. Zain Elabedien and E.-Z.M. Ebeid, *Int. J. Biol. Macromol.*, **233**, 123562 (2023); https://doi.org/10.1016/j.ijbiomac.2023.123562
17. B. Ahmad and J. Ali, *Afr. J. Pharm. Pharmacol.*, **7**, 375 (2013); https://doi.org/10.5897/AJPP12.1246
18. H. Groen and K.J. Roberts, *J. Phys. Chem. B*, **105**, 10723 (2001); https://doi.org/10.1021/jp011128l
19. A.A. Keirudin, N. Zainuddin and N.A. Yusof, *Polymers*, **12**, 2465 (2020); https://doi.org/10.3390/polym12112465
20. M.K. Liang, M.J. Limo, A. Sola-Rabada, M.J. Roe and C.C. Perry, *Chem. Mater.*, **26**, 4119 (2014); https://doi.org/10.1021/cm501096p
21. Z. Tian, Z. Guo, G. Duan, J. Han, W. Li, Y. Huang, X. Han, C. Zhang, S. He, H. Hou and S. Jiang, *Adv. Fiber Mater.*, **7,** 1859 (2025); https://doi.org/10.1007/s42765-025-00584-z
22. T. Taghipour, G. Karimipour, M. Ghaedi and A. Asfaram, *Ultrason. Sonochem.*, **41**, 389 (2018); https://doi.org/10.1016/j.ultsonch.2017.09.056
23. A. Patti, *Macromol. Rapid Commun.*, **46**, 2400636 (2025); https://doi.org/10.1002/marc.202400636
24. M. Wang, J. Kang, J. Yang, Z. Wen, M. Zhao and Z. Li, *J. Environ. Chem. Eng.*, **13**, 118707 (2025); https://doi.org/10.1016/j.jece.2025.118707
25. B.H. Dong and J.P. Hinestroza, *ACS Appl. Mater. Interfaces*, **1**, 797 (2009); https://doi.org/10.1021/am800225j
26. Y. Zhu, T. Mei, Y. Wang and Y. Qian, *J. Mater. Chem.*, **21**, 11457 (2011); https://doi.org/10.1039/c1jm11079a